

# **Robust Control for a 3DOF Articulated Robotic Manipulator Joint Torque under Uncertainties**

## **ABSTRACT**

This research work emphasizes on design of a robust control for a 3DOF robotic manipulator under uncertainties. The plant model was achieved using the independent joint method and the uncertainty problem was addressed by designing a robust controller using H-Infinity synthesis which was compared with PID. This was achieved with algorithms implemented in MATLAB. The H-Infinity controller recorded zero dB, while PID controller recorded 0.117dB and 0.061dB for joints I and II respectively in Complementary Sensitivity (T) graph at low frequencies. H-Infinity controller achieved better disturbance rejection characteristics with sensitivity (S) graph recording peak sensitivity of 0.817dB and 1.79dB at joints I and II respectively than PID controller which achieved 3dB and 1.86dB at joints I and II respectively. H-Infinity controller achieved better noise rejection characteristics with T graph recording lower gains of -220dB and -310dB at joints I and II respectively at high frequencies than PID controller which recorded -134dB and -153dB gains at joints I and II respectively. Thus, it was concluded that the H-Infinity controller achieved better performance and stability robustness characteristics for the joint torque control than the PID.

*Keywords: H-Infinity Synthesis, Joint Torque Control, PID, Robotic Manipulator, Robust Control, Uncertainty*

## **1. INTRODUCTION**

The robotic manipulator is a reprogrammable mechanical arm, moved or controlled by actuators to perform similar functions to human arm. It is a physical system with many subsystems such as the mechanical, electrical and electronics, etc. These subsystems are in most cases non-negligible in the mathematical description of the robotic manipulator. If there is one technological advancement that would certainly make living easy and convenient, robots would be the answer. They have shown significance in decreasing human work load especially in industries by making works easy and convenient. Robots are mostly utilized in the manufacturing industry where they usually provide solutions to repetitive and monotonous works which are normally problems to human workers.

Manipulators consist basically of links connected together by joints, and it is usually classified based on the first three joints of the arm, with the wrist being described separately. Two common types of joint: Revolute (R) and Prismatic (P). The majority of the industrial manipulators fall into one of five geometric types: articulated (RRR), spherical (RRP), SCARA (RRP), cylindrical (RPP), or Cartesian (PPP). Articulated robotic manipulators consist of revolute joints which are basically controlled by electric motors. They are very flexible and dexterous to fit into many fields of work such as medical surgeries, welding, painting, material handling, under water work etc.

The mathematical model of the robotic manipulator is a kinematical or dynamical description of the system. It is an important tool used in the development and improvement of the system. The Kinematics is the motion geometry of the robotic manipulator from the reference position to the desired position with no regard to forces or other factors that influence robot motion [1]. It is important in practical application such as trajectory planning [2]. Dynamics of the manipulator studies the motion of bodies (linkages) with consideration of the forces that cause the motion. It is important in the manipulator development, and also in the **joint torque control**. The torque and motion analysis of the mechanical arm requires only the link dynamics and the applied torque for the dynamic model and it is derived using Lagrange-Euler,

Newton Euler, D'Alembert in [3], while the joint torque control requires the dynamics of the actuator plus the links which is derived using the independent joint torque control approach.

Robotic manipulators are highly nonlinear dynamic systems with unmodeled dynamics and other uncertainties [4]. Uncertainties occur due to the discrepancy between the manipulator and its mathematical model representation, and disturbance signals. The performance of the manipulator is affected by the effects of the uncertainties in the system. In order to cancel these effects of uncertainties, a robust controller is introduced. Many research works have been done on the robust controllers development and from the review, the most common research gap is the failure to satisfy the robustness design specifications. Dorf and Bishop [5] stated that a system is robust when it has low sensitivity, it is stable over the range of parameter variation and performance continues to meet the specification in the presence of a set of changes in the system parameters. Hence, robustness is the minimized sensitivity to effects that are not considered in the analysis and design phase.

Robust controller design requires both robustness against model uncertainty, as well as good disturbance and noise rejection characteristics and good performance. Considerable advancements in control system design led to the introduction of H-Infinity ( $H_\infty$ ) synthesis. This approach makes use of weights to achieve desired robustness and performance characteristics loop shape for the controller design. There are many advantages of this method such as high disturbance rejection, high stability and many more [6]. The H-Infinity synthesis technique and PID (proportional-Integral-Derivative) control scheme were applied and compared for the design of the robust controller.

## 2. LITERATURE REVIEW

The dynamic model presented in [7-10] is basically the dynamical description of the mechanical arm of the manipulator. Kim and Lee [11] proposed a robust control model of robotic manipulators under parametric uncertainty using only robot link dynamic model based on the Lagrange-Euler equation of motion of robot links. This method of robot dynamic model was used in many research works but recently, it has been criticized in Fateh [12], due to its limitations in feedback application and drawback in its application to the actuator inputs. The model is mostly used for the applied torque and motion analysis. Secondly, friction vector was not included in their dynamic model. Biradar et al [13] investigated Lagrange-Euler method and suggested that there should be an improved model that can be implemented in the controller of the manipulator, and optimized for a specific job task. In Izadbakhsh et al [14], the Lagrange model was used when considering the equation of motion of robot links. Lewis et al [15] stated that to obtain a complete dynamical description of the arm plus the actuator (which make up the robotic manipulator), it is required to add the actuator dynamics to the arm dynamics. Talole et al [16] proposed a mathematical model of a single rigid link manipulator based on the link (or arm) dynamics plus the actuator dynamics. In [17] actuator model was computed and merged with the dynamic model of the robot arm. In [18] an articulated robotic manipulator was modeled based on the actuator model for controller design. In [12] the manipulator was modeled based on independent joint method which is based on the joint actuator dynamic model and the torque due to link. According to him, using this method obtains simplicity, accuracy, speed of calculation and robustness to the manipulator control system. In [19] an articulated robot manipulator was modeled for precise positioning using joint actuator dynamic model instead of the Lagrangian-Euler robot model of the arm. The controller design for the robotic manipulator in [20] was based on joint actuation (i.e., the joint actuator model) which was carried out independently. From the review, for controller design, the joint actuator dynamics should be merged with robot arm dynamics at the pivot.

In the robust control methods the controller is designed based on the plant mathematical model. Since the controller design objective is to be able to cancel the effects of possible uncertainty that exists or may arise in the system hence, assuming uncertainty bounds for the controller design limits the robustness capability of the controller when implemented. In order to achieve a robust system therefore, the controller is designed based on the robustness specifications and analysis [21]. Uncertainty can be in any parameter, such as the load carrying by the end effector [22]. Many researchers have proposed and developed many methods of achieving a robust controller. The major goal of the robust controller design is to obtain controller gains that can achieve the desired output trajectory in the presence of significant uncertainties. This is achieved by designing a controller that satisfies the robust control specifications. Ahuja and Tandon [23] presented a robust PID and Polynomial controllers for DC motor speed control. The uncertainty caused by the parameter changes of motor resistance, motor inductance and load are formulated in their work as multiplicative uncertainty weight, which were used in the objective function in the design.

Bansal and Sharma [6] applied  $H_\infty$  synthesis in their work for robust controller design. They stated that  $H_\infty$  control synthesis is found to guarantee robustness and good performance and also provides high disturbance rejection. Baslamish [24] applied  $H_\infty$  controller in Linear Parameter Varying (LPV) Modeling and Robust Control of Yaw and Roll Modes of Road Vehicles. Yadav and Singh [25] carried out a design on the robust control of two link rigid manipulator. In their work, H-Infinity controller design method was applied and it achieved good system performance and robustness.

However, the controller results showed high system overshoot. Wang et al [8] carried out a research work on robust tracking control of robotic manipulator using dissipativity theory based on  $H_\infty$  controller technique. It was confirmed in their work that the scheme improved the robustness of the system.

### 3. METHODOLOGY

The robotic manipulator often times comprises of basically the arm (links), joints actuators, gears and a controller for each joint. The arm is a mechanical setup of mainly the links. It can be described dynamically using the Lagrange-Euler method as stated in [26]:

$$M(q)\ddot{q} + C(q, \dot{q})\dot{q} + G(q) = \tau \quad (1)$$

Where  $\tau$  is actuation torque,  $q$  is the joint variable vector,  $M(q)$  is the completed inertia matrix,  $C(q, \dot{q})\dot{q}$  is the centripetal and Coriolis torque vector,  $g(q)$  is the gravitational torque vector. This equation describes only the dynamics of the robot arm and therefore cannot be applied for to the actuators for torque control law development.

The dynamic equation of a manipulator driven by DC motors [27] is formulated as follows:

$$M(q)\ddot{q} + C(q, \dot{q})\dot{q} + g(q) = K_t i \quad (2)$$

where  $i$  is the armature current vector, and  $K_t$  is the diagonal matrix of motor torque constant. The torque generated by the actuator is related to the actuator current as follows:

$$\tau_m = K_t i \quad (3)$$

Sum of torques at the actuator gear is equal to zero, that is:

$$J_m \frac{d^2 \theta_m}{dt^2} + B_m \frac{d \theta_m}{dt} = K_t i \quad (4)$$

The electrical circuit of the actuator provides the equation [12, 28]:

$$V_{in} = Ri + L_a \frac{di}{dt} + K_e \frac{d \theta_m}{dt} \quad (5)$$

The manipulator is made up of links connected together by joints and each joint consists of actuator and gears (motor and link gears) connecting the arm to the joint as shown in figure 1a. Figure 1b shows the 2D diagram of the 3DOF manipulator. Since the control law for the joint torque control is applied to the actuator through the controller thus, a complete dynamic model of the system must consists of the robot arm dynamics plus the actuator dynamics for the controller design. In order to achieve a model to design the controller the dynamics of both the actuator and link are coupled at the gears using the independent joint scheme based on Single Input Single Output (SISO). The 3DOF robotic manipulator model is explained in details in [29]:

$$\begin{cases} \left( \frac{r_l}{r_m} J_m + \frac{r_m}{r_l} J_l \right) s^2 q + \left( \frac{r_l}{r_m} B_m + \frac{r_m}{r_l} B_l \right) s q = K_t I \\ V_{in} = RI + L_a s I + \frac{r_l}{r_m} K_e \dot{q} \end{cases} \quad (6)$$

The dynamic model for joint torque control relating angular position of the link and the voltage input into the actuator becomes:

$$G_P = \left( s \left[ \left( \frac{r_l}{r_m} J_m + \frac{r_m}{r_l} J_l \right) s + \left( \frac{r_l}{r_m} B_m + \frac{r_m}{r_l} B_l \right) \right] (L_a s + R) + K_e K_t \right)^{-1} K_t \quad (7)$$

$$q = \left( s \left[ \left( \frac{r_l}{r_m} J_m + \frac{r_m}{r_l} J_l \right) s + \left( \frac{r_l}{r_m} B_m + \frac{r_m}{r_l} B_l \right) \right] (L_a s + R) + K_e K_t \right)^{-1} K_t V(s) \quad (8)$$

Simplifying the joint mechanical subsystem dynamics yields:

$$\begin{cases} J_T \ddot{q} + B_T \dot{q} = \tau \\ V_{in} = RI + L_a s I + \frac{r_l}{r_m} K_e \dot{q} \end{cases} \quad (9)$$

Where  $J_T = \frac{r_l}{r_m} J_m + \frac{r_m}{r_l} J_l$  is the total inertia at the joint and  $B_T = \frac{r_l}{r_m} B_m + \frac{r_m}{r_l} B_l$  is the total torsional viscous damping coefficient

Where  $G_P$  is the plant transfer function

#### 3.1 Robust Control Model

Under external disturbances and plant uncertainties, the true mechanical dynamics of the complete torque control model are assumed to be:

$$J\ddot{q} + B\dot{q} = \tau - D(q, \dot{q}, t) \quad (10)$$

Where  $J = J_T + \Delta J$ ,  $B = B_T + \Delta B$ , and  $D(q, \dot{q}, t)$  is the disturbance input such as unmodeled dynamics. The model can be represented as:

$$\begin{aligned} (J_T + \Delta J)\ddot{q} + (B_T + \Delta B)\dot{q} &= \tau - D(q, \dot{q}, t) \\ \ddot{q} &= (J)^{-1}(\tau - B\dot{q} - D(q, \dot{q}, t)) \end{aligned} \quad (11)$$

Ignoring the uncertainty, the model becomes

$$\ddot{q}_d = (J_T)^{-1}(\tau - B_T \dot{q}) \quad (12)$$

The difference between the desired  $\ddot{q}_d$  and actual joint variables  $\ddot{q}$  is the error model  $e$  or model uncertainty, in the system.

$$e = -\ddot{q}_d + (J)^{-1}(\tau - B\dot{q} - D(q, \dot{q}, t)) \quad (13)$$

The influences of the nonlinearities, unmodeled and neglected dynamics in the model are treated as disturbances and the controller is designed to be robust against them [29].

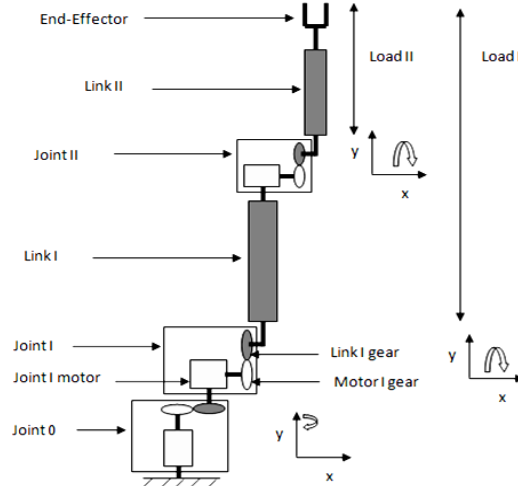


Fig 1a: Internal structure of the 3DOF articulated robotic manipulator

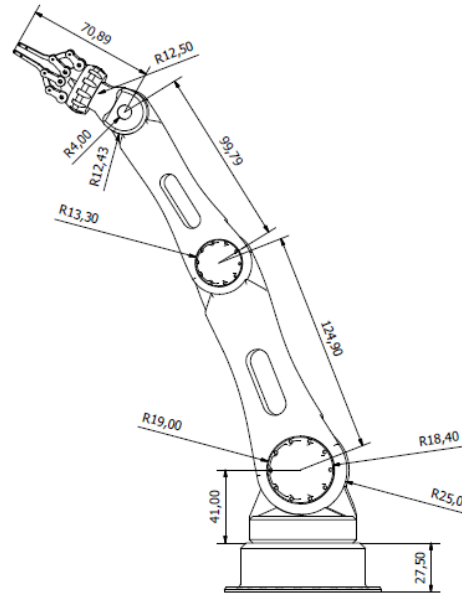


Fig 1b: 3DOF Robot arm 2D structure and dimensions

### 3.2 Robust Controller Design

Considering the manipulator in a real environment in figure 2a with uncertainties, the inputs to the system become the reference input  $r$ , the disturbance  $D$ , and measurement noise  $N$ .

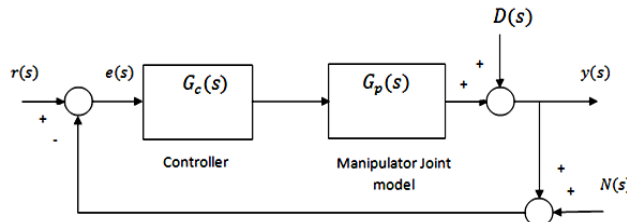


Fig 2a: Control system with disturbance and noise inputs in real environment

The general transfer function of the feedback controlled system is represented as follows:

$$y(s) = \frac{G_c(s)G_p(s)}{1+G_c(s)G_p(s)}(r(s) - N(s)) + \frac{1}{1+G_c(s)G_p(s)}D(s) \quad (14)$$

$$y(s) = \frac{G_c(s)G_p(s)}{1+G_c(s)G_p(s)}r(s) - \frac{G_c(s)G_p(s)}{1+G_c(s)G_p(s)}N(s) + \frac{1}{1+G_c(s)G_p(s)}D(s) \quad (15)$$

$$e(s) = \frac{1}{1+G_c(s)G_p(s)}(r(s) - D(s) + N(s)) \quad (16)$$

From equation 14, the following functions are derived

$$T(s) = \frac{G_c(s)G_p(s)}{1+G_c(s)G_p(s)}, S(s) = \frac{1}{1+G_c(s)G_p(s)}, L(s)G_p(s) = Lg(s)$$

T(s) (i.e. complementary sensitivity function) is the transfer function between the output and the reference input of the system through the feedback. S(s) (i.e. Sensitivity function) is the transfer function between the output and disturbances of a system. Lg(s) is the open loop function.

The robust controller design is based on shaping the sensitivity and complementary sensitivity transfer functions graphs to the desired shape. The singular value plot for S and T for robustness analysis in [31] was simplified and modified in figures 2b and 2c.

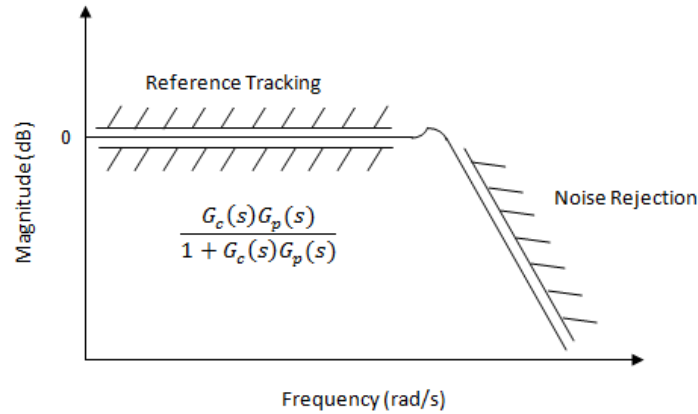


Fig 2b: Complementary sensitivity (T) graph

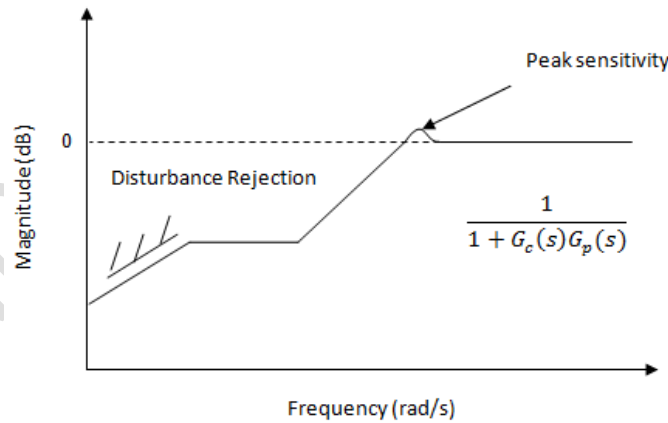


Fig 2c: Sensitivity (S) graph

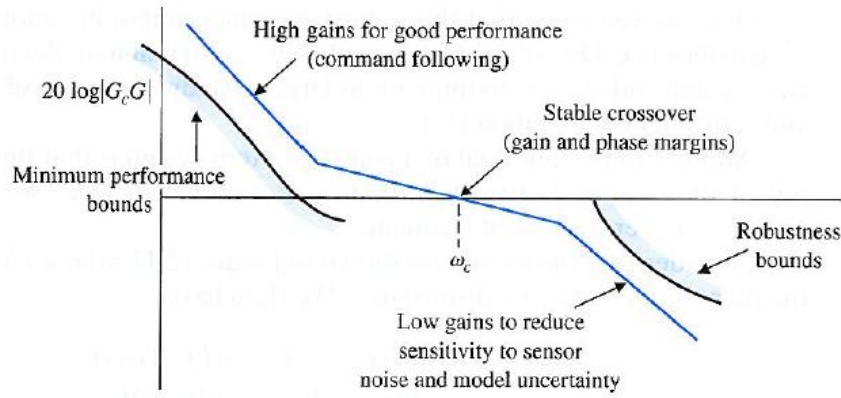


Fig 2d: Demonstration of system behavior on Bode plot [5]

The following objectives must be met for the system to achieve full robustness characteristics.

- For good set-point tracking (i.e., system output performance)  $|T(j\omega)|$  must follow the zero gain line at low frequencies.
- For good disturbance rejection,  $S(s)$  or  $|S(j\omega)| \ll 1$
- For good noise suppression,  $|T(j\omega)| \ll 0$  at frequencies of noise
- For robust stability, Gain margin must be greater than or equal to 20dB
- For robust stability, Phase margin must be greater than or equal to 60degree
- Open loop peak gain must be very much greater than 0dB for good performance (figure 2d)
- $|Lg(j\omega)| \ll 0$  at high frequencies to reduce noise and model uncertainties

### 3.3 H-Infinity Controller Design

The In-Infinity controller design method here involves the control of the joint models with the developed weights  $W1$  and  $W2$  base on the joint parameters. The weight parameters are varied in order to improve the iteration results. The weighting functions have been chosen according to industrial performance specifications in [30].

**Wp (W1):** the inverse of the weighting function  $Wp(s)$  is used to impose a performance specification in terms of the sensitivity function  $S$ .  $Wp$  is chosen:

$$Wp(s) = \frac{s/M_s + w_b}{s + w_b * A_s} \quad (17)$$

where  $M_s$  is to introduce a margin of robustness on the peak of  $S$ ,  $w_b$  helps to have a sensible attenuation of disturbances and  $A_s$  helps to reduce the steady-state position error.

**Wu (W2):** the control output  $u$  is weighted according to the actuator limitations.  $Wu(s)$  is set to:

$$Wu(s) = \frac{s + \omega_{bc}/M_u}{s * \epsilon + \omega_{bc}} \quad (18)$$

where  $M_u$  helps to impose limitations on the maximum value of the controller output signal,  $w_{bc}$  helps to limit the effect of measurement noise and plant uncertainties at high frequencies, and  $\epsilon$  helps to ensure a high-frequency controller gain.

#### Proposed H-Infinity Synthesis Algorithm:

- Establish the joint model  $G(s)$  for joint I and II
- Apply weight  $W1$  to control the joint sensitivity to disturbance
- Apply moderate control  $W2$  on the control signal  $u$
- Ignore the closed loop system ( $T$ ) control by applying no control,  $W3=0$
- Augment or connect the plant  $G(s)$  with weighting functions  $W1(s)$ ,  $W2(s)$  and  $W3(s)$  (design specifications) to form an "augmented plant"  $P(s)$
- Apply H-Infinity synthesis for loop shaping and generate  $K$  (controller model)
- Form the loop gain ( $Lg$ ) =  $K * P$
- Form the system sensitivity function  $S = (1 + Lg)^{-1}$
- Form  $T$ ,  $(1 - S)$
- Analyze  $Lg$ ,  $S$  and  $T$  for performance and robustness of the controlled system

This technique allows very precise loop shaping via suitable weighting strategies and thereby achieves robust control.

### 3.4 Proportional-Integral-Derivative (PID) Controller Design

The proportional-integral-derivative controller algorithm is derived as follows:

$$U(t) = K_p e(t) + K_I \int e(t) dt + K_D \frac{d}{dt} e(t) \quad (19)$$

Applying Laplace transformation;

$$U(s) = K_p e(s) + K_I \frac{1}{s} e(s) + K_D s e(s) \quad (20)$$

$$U(s) = (K_p + K_I \frac{1}{s} + K_D s) e(s) \quad (21)$$

$$G_c(s) = K_p + K_I \frac{1}{s} + K_D s \quad (22)$$

Generating the loop gain of the controlled system for robust control analysis:

$$Lg(s) = (K_p + K_I \frac{1}{s} + K_D s) G_p \quad (23)$$

#### Proposed PID Controller Design Algorithm:

- Establish the joint model  $G(s)$  for joint I and II,
- Select the controller gains with the help of PID tuner in MATLAB
- Form the controller model with the gains
- Form the loop gain  $(Lg) = K \cdot P$
- Form the system sensitivity function  $S = (1 + Lg)^{-1}$
- Form  $T, (1 - S)$
- Analyze  $Lg, S$  and  $T$  for performance and robustness of the controlled system

System parameters for the simulation experiments are as presented in table 1. The experiments were carried out for the joints I and II separately based on their respective parameters.

Table 1: Manipulator joint parameters

| Parameters                        | Joint I                | Joint II                |
|-----------------------------------|------------------------|-------------------------|
| Inertia (J)                       | 0.001Kg-m <sup>2</sup> | 0.0003Kg-m <sup>2</sup> |
| Resistance (R)                    | 3Ω                     | 4Ω                      |
| Inductance ( $L_a$ )              | 0.004H                 | 0.002H                  |
| Torque Constant (kt)              | 0.1N.m/A               | 0.05N.m/A               |
| Electromotive Force Constant (Ke) | 0.1V.s/rad             | 0.05V.s/rad             |
| Viscous Damping Coefficient       | 0.0001                 | 0.01                    |

## 4. RESULTS AND DISCUSSIONS

Figures 3 and 4 show the sigma plot of  $Lg, S$  and  $T$  function graphs of the PID and H-Infinity controllers respectively for joint I and this was repeated for joint II as shown in figures 5 and 6. The results from the sigma plots were summarized in tables 2 and 3. The sigma plots show the behaviors of the controlled system which helped to determine the robustness and performance characteristics.

The H-Infinity controller was achieved by varying the values of the weights to determine the best performance and robustness loop shape of the three functions for each robot joint. For the Joint I, the following weights were used:

$$W1 = \frac{0.1(s+100)}{s+0.1}, W2 = 1/(s + 100), W3 = 0$$

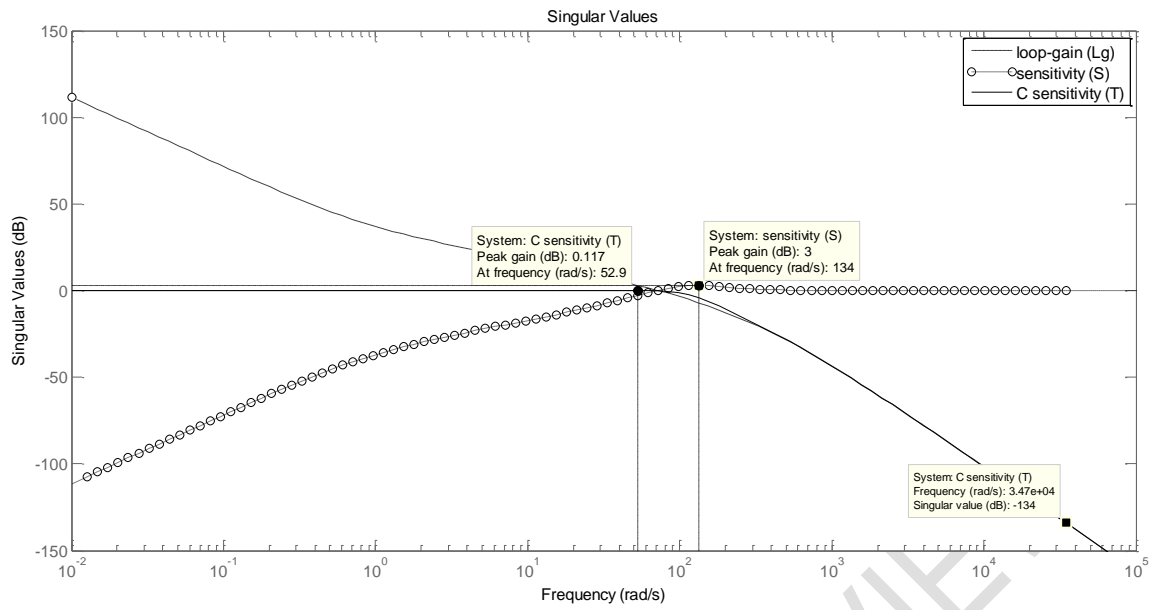


Fig 3: Sigma plot of Lg, S and T for PID controlled joint I

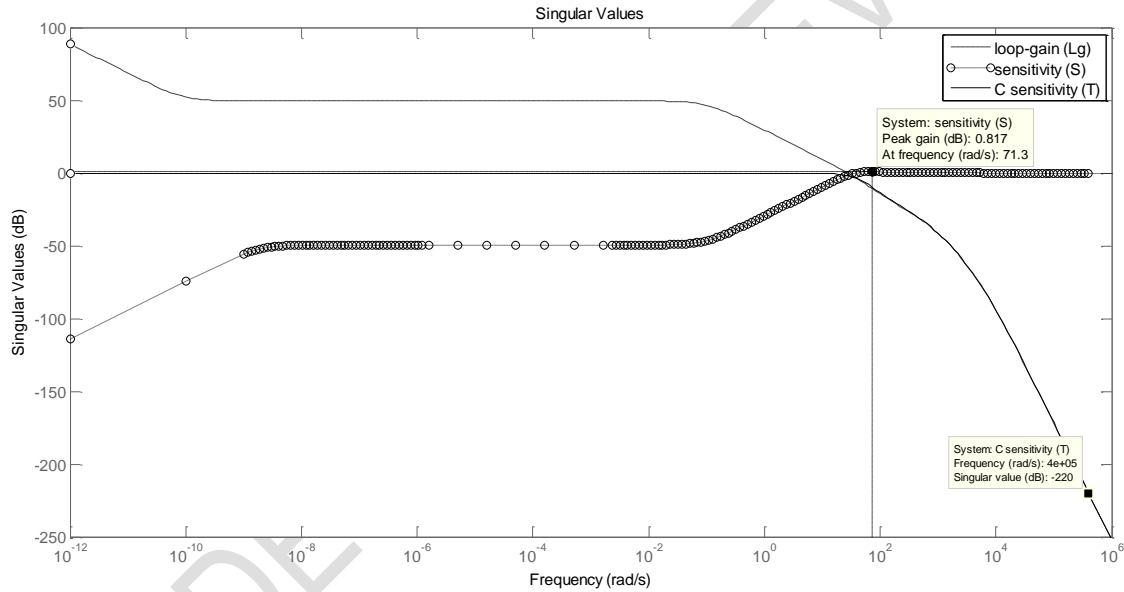


Fig 4: Sigma plot of Lg, S and T for H-Infinity controlled joint I



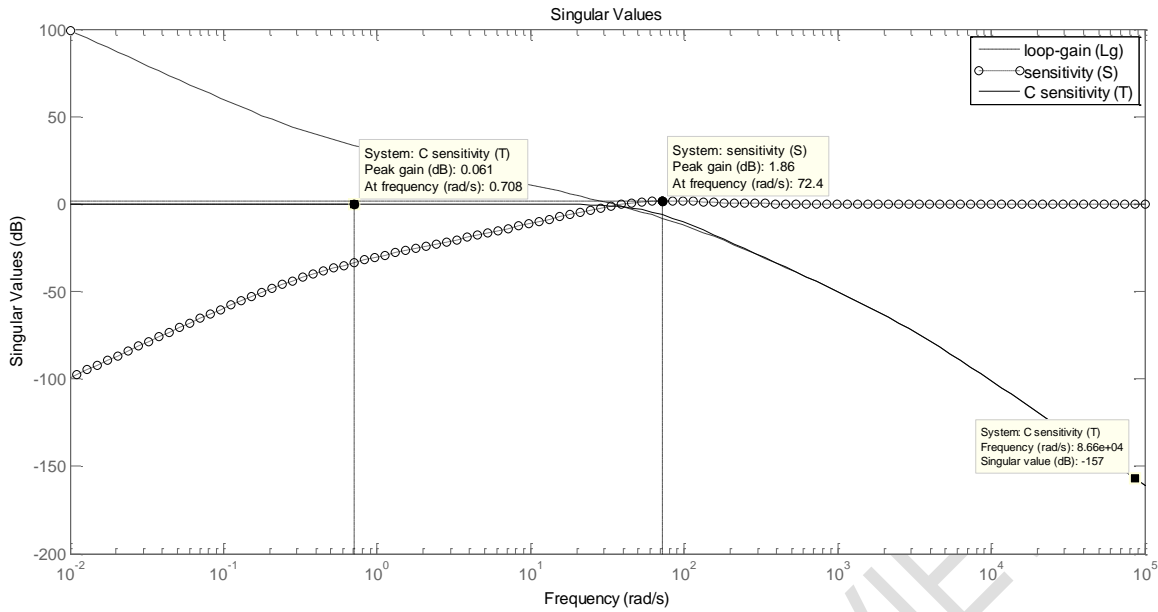


Fig 5: Sigma plot of Lg, S and T for PID controlled joint II

Table 2: Summary of PID and H-Infinity controller results for joint I

| Parameter                                   | PID   | H-Infinity |
|---|-------|------------|
| Complementary sensitivity at high frequency | -134  | -220       |
| System sensitivity at low frequency         | -107  | -114       |
| Peak Sensitivity                            | 3     | 0.817      |
| Overshoot                                   | 7.27  | 0.62       |
| Reference tracking error                    | 0.117 | 0          |
| Gain margin                                 | 20.4  | 43.6       |
| Phase margin                                | 60.1  | 75.1       |

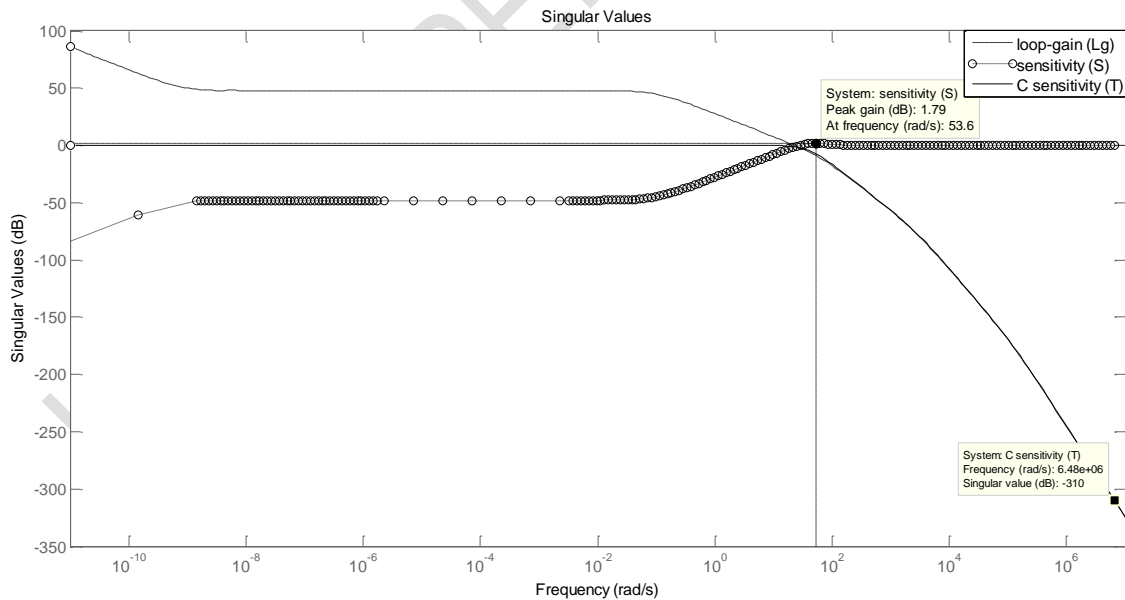


Fig 6: Sigma plot of Lg, S and T for H-Infinity controlled joint II

For the Joint II, the following weights were used:  $W1 = \frac{s+100}{s+0.1}$ ,  $W2 = 0.1$ ,  $W3 = 0$

Table 3: Summary of the PID and H-Infinity controllers results for joint II

| Parameter                                   | PID  | H-Infinity |
|---|------|------------|
| Complementary sensitivity at high frequency | -153 | -310       |

|                                     |       |       |
|-------------------------------------|-------|-------|
| System sensitivity at low frequency | -97.4 | -82.9 |
| Peak Sensitivity                    | 1.86  | 1.79  |
| Overshoot                           | 1.86  | 1.17  |
| Reference tracking error            | 0.061 | 0     |
| Gain margin                         | 37.9  | 41.1  |
| Phase margin                        | 69    | 69.8  |

From the results in tables 2 and 3, the H-Infinity recorded the best performance and stability robustness characteristics with lower values of peak sensitivity, overshoot, and steady state error in both joints 1 and 2 compared with the PID controllers.

The robust controllers designed for the robotic manipulator joint I and II torque control were expressed in a transfer function equations as follows:

$$K_{Joint1} = \frac{7627984s^4 + 5970009760s^3 + 676138569601s^2 + 42109050879999s + 2415781888001150}{s^5 + 11700.1s^4 + 26977169.18s^3 + 12323975711.74s^2 + 308047269564.02s + 30660460014.33}$$

$$K_{Joint2} = \frac{5141604s^3 + 14140164480.07s^2 - 327455231999.56s - 22228377599996.57}{s^4 + 132400.1s^3 + 364300838.83s^2 + 22492925007.38s + 2178259942.85}$$

## 5. CONCLUSION

The mathematical model for robotic manipulator joint torque control being one of the major problems of the system was achieved using the independent joint technique. This method provides a simpler plant model which can easily be implemented in the controller development and also in practical realization of the manipulator. Robust controller for an articulated robotic manipulator joint torque control was developed using H-Infinity synthesis method and compared with the PID design method. From the results, the T graph at low frequencies for H-Infinity controller recorded zero dB line at joint I and II, while for PID controller it recorded 0.117dB and 0.061dB for joints I and II respectively. Therefore, the H-Infinity achieved better performance characteristics than PID. The sensitivity S graph for H-Infinity achieved peak sensitivity of 0.817dB and 1.79dB at joints I and II respectively while it achieved 3dB and 1.86dB at joints I and II respectively for PID controller. Thus, the H-Infinity controller achieved better disturbance rejection characteristics than PID controller. From the T graph, the H-Infinity recorded lower gains of -220dB and -310dB at joints I and II respectively at high frequencies than the PID which recorded -134dB and -153dB gains at joints I and II respectively at high frequencies. Therefore, H-Infinity controller achieved better noise rejection characteristics than the PID controller. It was hence concluded that the H-Infinity controller achieved better performance and robustness characteristics for the joint torque control.

This work optimizes the performance of the joint torque control of the manipulator by applying the H-Infinity controller. This method improves the robustness of the system by achieving reduced or low sensitivity and good disturbance rejection characteristics while maintaining robust stability. Hence, the H-Infinity controller design method is recommended for the control of autonomous robots (humanoids), Remotely Operated Vehicles (ROVs), and Unmanned Aerial Vehicles (UAMs) etc. Since, it has been noted that building humanoid robots that can do useful things in the real world, not just research labs, is very difficult [32] due to its complex nature, independent joint scheme and robust control are therefore recommended for such works.

Further work should be carried out on the area of hybridizing the PID and H-Infinity controllers for better performance and robustness of the system.

## COMPETING INTERESTS

There is no competing interest.

## REFERENCES

1. J.J. Grage, Introduction to Robotics Mechanics and Control, 3<sup>rd</sup> Ed, Prentice Hall, (2005).
2. A.Z. Alassar, Modeling and Control of 5DOF Robot Arm using Supervisory Control, University of Gaza, pp.1-105, (2010).
3. V. Filip Dynamic Modeling of Manipulators with Symbolic Computational Method, The Publishing House of the Romanian Academy, Proceedings of the Romanian Academy, Series A, Vol. 9, Num. 3, pg.1, (2008).

4. X. Ren, A. Rad, F. Lewis, Neural network-based compensation control of robot manipulators with unknown dynamics, in: American Control Conference, 2007. ACC'07, pp. 13–18, (2007).
5. R.C. Dorf, and R.H. Bishop, Modern Control Systems, Pearson Prentice Hall, 11<sup>th</sup> Ed., (2008).
6. A. Bansal and V. Sharma, Design and Analysis of Robust H-infinity Controller, Control Theory and Informatics, Vol.3, No.2, pp.7-14, (2013).
7. C.S. Liu and H. Peng, Disturbance Observer Based Tracking Control, Journal of Dynamic Systems, Measurement, and Control, Vol. 122, pp. 332-335, (2000).
8. H. Wang, Z. Feng, and X. Liu, Robust Tracking Control of Robot Manipulator Using Dissipativity Theory, Modern Applied Science, Vol. 2, No. 4, Pg. 95, (2008).
9. K. Lochan, and B.K. Roy, Control of Two-link 2-DOF Robot Manipulator Using Fuzzy Logic Techniques: A Review, Springer India, pp. 499-511, (2015).
10. J. Liu and R. Liu, Simple Method to the Dynamic Modeling of Industrial Robot Subject to Constraint, Advances in Mechanical Engineering, Vol. 8(4) pg.4, (2016).
11. C.S. Kim, and K.W. Lee, Robust Control of Robot Manipulators using Dynamic Compensators under Parametric Uncertainty, International Journal of Innovative Computing, Information and Control, Vol. 7, No. 7, pp.4129-4137, (2011).
12. M.M. Fateh, On the Voltage-Based Control of Robot Manipulators, International Journal of Control, Automation and Systems, Vol. 6, No. 5, pp. 702-712, (2008).
13. R. Biradar and M.C. Kiran, The Dynamics of Fixed Base and Free-Floating Robotic Manipulator, International Journal of Engineering Research & Technology (IJERT), Vol. 1 Iss. 5, pg. 1, (2012).
14. A. Izadbakhsh, and M.M. Fateh, A Model-Free Robust Control Approach for Robot Manipulator, World Academy of Science, Engineering and Technology, (2007).
15. F.L. Lewis, D.M. Dawson, C.T. Abdallah, Robotic Manipulator Control, Theory and Practice, Marcel Dekker Inc., New York, 2<sup>nd</sup> Ed. Pg. 152-158, (2004).
16. S.E. Talole, S.B. Phadke and R.K. Singh, Robust Feedback Linearization Based Control of Robot Manipulator, Institute of Armament Technology, Girinaga, Pune, India, pg. 89
17. K.M. Helal, M.R.A. Atia, M.I.A. El-Sebah, Gain Scheduling Control with Multi-Loop PID for 2-DOF Arm Robot Trajectory Control, IRES 23rd International Conference, Dubai, UAE, Pg.19, (2015).
18. R. Agrawal, K. Kabiraj, R. Singh, Modeling a Controller for an Articulated Robotic Arm, Scientific Research, Intelligent Control and Automation, Vol. 3, pp.207-210, (2012).
19. E.G. Ovy, S. Seeraji, S.M. Ferdous, M. Rokonzaman, A Novel Design of an ATmega32L Microcontroller Based Controller Circuit for the Motion Control of a Robot Arm Actuated by DC Motors, Cyber Journals: Journal of Selected Areas in Robotics and Control (JSRC), April Edition, pp.1-8, (2011).
20. T. Liu Design And Prototyping of a Three Degrees of Freedom Robotic Wrist Mechanism for a Robotic Surgery System, Case Western Reserve University, pp.1-83, (2011).
21. E.C. Agbaraji, Robustness Analysis of a Closed-loop Controller for a Robot Manipulator in Real Environments, Physical Science International Journal, 8(3): 1-11, (2015).
22. H.A.H. Alashqar, Modeling and High Precision Motion Control of 3 DOF Parallel Delta Robot Manipulator, The Islamic University of Gaza pp.1-98, (2007).
23. A. Ahuja, and B. Tandon, Robust PID and Polynomial Controllers Tuning for DC Motor Speed Control using PSO and GA: a Comparative Study, International Journal of Electrical and Electronics Engineering Research (IJEER), Vol.3, Iss. 1, pp.273-286, (2013).
24. S.C. Baslamish, LPV Modeling and Robust Control of Yaw and Roll Modes of Road Vehicles, (2007), Retrieved on October 19, 2016 from: <http://yunus.hacettepe.edu.tr/~scaglarb/PHD/tezim6.pdf>
25. P.S. Yadav, and N. Singh, Robust Control of Two Link Rigid Manipulator, International Journal of Information and Electronics Engineering, Vol. 5, No. 3, pp.198-203, (2015).
26. L. Cheng, Z.G. Hou, M. Tan, D. Liu, and A.M. Zou, Multi-agent based adaptive consensus control for multiple manipulators with kinematic uncertainties, pp.189-194, (2008).
27. M.W. Spong, S. Hutchinson, and M. Vidyasagar, Robot Modeling and Control, John Wiley & Sons, Inc., 1<sup>st</sup> Ed, (2006).
28. M.W. Spong and M. Vidyasagar, Robot Dynamics and Control, John Wiley & Sons, Inc., 1<sup>st</sup> Ed, (1989).
29. E.C. Agbaraji, H.C. Inyama, and C.C. Okezie, Dynamic Modeling of a 3-DOF Articulated Robotic Manipulator Based on Independent Joint Scheme, Physical Science International Journal, 15(1): 1-10, (2017)
30. G. Filardi, O. Sename, A.B. Voda, H.J. Schroeder, Robust H-Infinity Control of A DVD Drive Under Parametric Uncertainties, Paper ID: 632, pp.1-6
31. S.S. Nair, Automatic Weight Selection Algorithm for Designing H Infinity controller for Active Magnetic Bearing, International Journal of Engineering Science and Technology (IJEST), Vol. 3, No. 1, pp. 122-138, (2011)
32. S. Crowe, Humanoid robots: Five to watch in 2019, WTWH Media, LLC, (2019)